RSC Advances

PAPER

Cite this: *RSC Adv.*, 2019, **9**, 41240

Stable and sensitive amino-functionalized graphene/polyaniline nanofiber composites for room-temperature carbon dioxide sensing

Hanan Abdali, [ab] Bentolhoda Heli [a] and Abdellah Ajji*[a]

Received 10th August 2019
Accepted 28th November 2019

DOI: 10.1039/c9ra06223h

rsc.li/rsc-advances

This article describes the preparation and characterization of amino-functionalized graphene (AmG)/polyaniline (PANI)/poly(methyl methacrylate) (PMMA) nanofiber mats along with the efficiency of these nanofiber composites as a new material for sensing carbon dioxide (CO_2) gas. The surfaces of the PMMA nanofibers were treated at room temperature by ultraviolet (UV) radiation. AmG/PANI was then deposited on the surfaces of the PMMA nanofibers *via* chemical oxidative polymerization. It was concluded that UV radiation reduced the hydrophobicity of the PMMA surface through introducing oxidized groups onto the surface. The electrical response of the gas sensor based on the composite nanofibers was investigated at room temperature using various concentrations of CO_2 gas. Compared to the PANI/PMMA nanofibers, the AmG/PANI nanofiber composites displayed a better electrical resistance response to CO_2 at room temperature; the AmG/PANI nanofiber composites exhibited higher sensitivity and faster response times under the same conditions.

Introduction

Carbon dioxide (CO_2) is used in a numerous areas such as analytical chemistry, environmental processes, medical diagnoses, and industrial processing. Air pollution is a worldwide concern, and the continuous increase of CO_2 in the atmosphere contributes to global warming, resulting in melting glaciers and the associated rise in sea levels.[1] Moreover, human exposure to high concentrations of CO_2 in the ambient environment causes suffocation and unconsciousness. Thus, researchers are interested in monitoring CO_2 levels in both the ambient (outdoor) and household (indoor) environments.[2–4] Gas sensors for CO_2 detection are typically based on the change in electrical responses upon exposure to CO_2.[5] As such, research to develop sensing materials has focused on manufacturing high-performance sensing materials and increasing the efficiencies of gas-sensing elements using materials capable of detecting abnormal concentrations of CO_2 in the atmosphere.[5] Therefore, a variety of materials have been considered for application in gas sensors, including inorganic semiconductors, metal oxides, dyes, conducting polymers, and carbon nanomaterials.[6–9] Among these sensing materials, graphene, a two-dimensional monolayer of carbon atoms, has been identified as a promising sensing material owing to its exceptional chemical and electronic properties, mechanical stiffness, and electrical conductivity,[10–12] which are desirable properties for fabricating resistive-type CO_2 gas sensors. Research on graphene has focused on understanding the extensive range of electronic, optical, thermal, and mechanical properties of graphene materials.[10–13] Nevertheless, numerous features of graphene can only be exploited when the graphene is integrated into more complex assemblies.[14,15] The chemical functionalization of graphene is the most common technique used to create these assemblies since it enables chemical bonding between graphene and the material of interest (*e.g.*, small molecules or polymer chains).[16–20] Moreover, the chemical functionalization of graphene is a particularly attractive because it can improve the solubility and processability of graphene.[21,22]

Graphene can be functionalized with organic, monomeric amines consisting of primary, secondary, or tertiary amine groups, which are known to be sensitive to CO_2 gas.[23] The binding of CO_2 to amino groups is based on the rule of hard and soft acids and bases.[24–26] CO_2 is a hard acid and can efficiently interact with the amino groups, which are hard bases, to form carbamates or bicarbonates, resulting in an increase in resistance.[24,25] In this work, we used ethylenediamine [NH_2–$(CH_2)_2$–NH_2] to functionalize the graphene surfaces, similar to in our previous work.[27] Many studies have demonstrated that primary amine groups are highly efficient in adsorbing CO_2 gas.[23–25] Therefore, in this work, the fundamental mechanism of CO_2 sensing is the efficient binding of amino-functionalized graphene with CO_2 at room temperature (RT) to form carbamates *via* a reversible reaction.

[a]*NSERC-Industry Chair, CREPEC, Department of Chemical Engineering, Polytechnique Montréal, P.O. Box 6079, Station Centre-Ville, Montreal, Quebec, H3C 3A7, Canada. E-mail: abdellah.ajji@polymtl.ca; Fax: +1-514-340-4159; Tel: +1-514-340-4711 ext. 3703*

[b]*Ministry of Education, P.O. Box 225085, Riyadh, 11153, Kingdom of Saudi Arabia*

Polyaniline (PANI) has been widely studied for gas detection based on its high sensitivity, fast response time, and functionality at room temperature.[7,28] However, the poor cycling stability of PANI-based sensors remains a significant obstacle for practical applications. However, the incorporation of conductive carbon materials can improve the cycle lifespan of PANI-based sensors. Combining the excellent sensing properties of amine-functionalized graphene (AmG) and PANI in an AmG/PANI composite is expected to enhance the stability, sensitivity, and selectivity of the resulting sensor. Poly(methyl methacrylate) (PMMA) is used in a wide range of nanotechnology applications. PMMA presents several advantages over other polymers in this study, including high mechanical strength, good thermal stability, nontoxicity, solubility in a variety of solvents, and good dielectric properties. These characteristics result in a polymer solution with good conductivity, which is favorable for electrospinning. Therefore, the sensitivity and recovery of the sensor could be improved *via* the *in situ* polymerization of AmG/PANI onto the surfaces of flexible electrospun PMMA substrates. The resulting nanofiber mats have an extremely high surface area-to-volume ratio and porosity, both of which are desirable properties in sensor applications.

Based on our literature survey in the field of composite-based nanofiber CO_2 sensors, no work has been reported on AmG/PANI nanofiber composite-based CO_2 sensors. In this study, PMMA nanofiber mats were produced *via* electrospinning and then treated with ultraviolet (UV) radiation at a wavelength of 365 nm. Subsequently, AmG/PANI were *in situ* polymerized on the surfaces of electrospun PMMA nanofibers to obtain flexible, composite nanofibers for CO_2 detection. The resulting AmG/PANI/PMMA sensor showed high sensitivity toward CO_2 gas at a concentration of 20 ppm. In addition, the response was reproducible for CO_2 gas concentrations ranging from 20 to 2000 ppm.

Results and discussion

Effect of UV treatment on substrate morphology

The SEM image in Fig. 1a shows the morphology of the neat PMMA nanofibers obtained from electrospinning. Nanofibers with smooth surfaces are randomly distributed in the membrane with relatively uniform sizes of 685 ± 220 nm. After the deposition of AmG/PANI by *in situ* polymerization (Fig. 1b), polymerization occurred only on the PMMA nanofiber surfaces and did not infiltrate the PMMA nanofibers due to the hydrophobicity of the PMMA nanofiber surfaces.[28,29] Therefore, the PMMA nanofibers were treated by UV radiation (wavelength = 365 nm) for 5 min (each side). UV radiation modified the

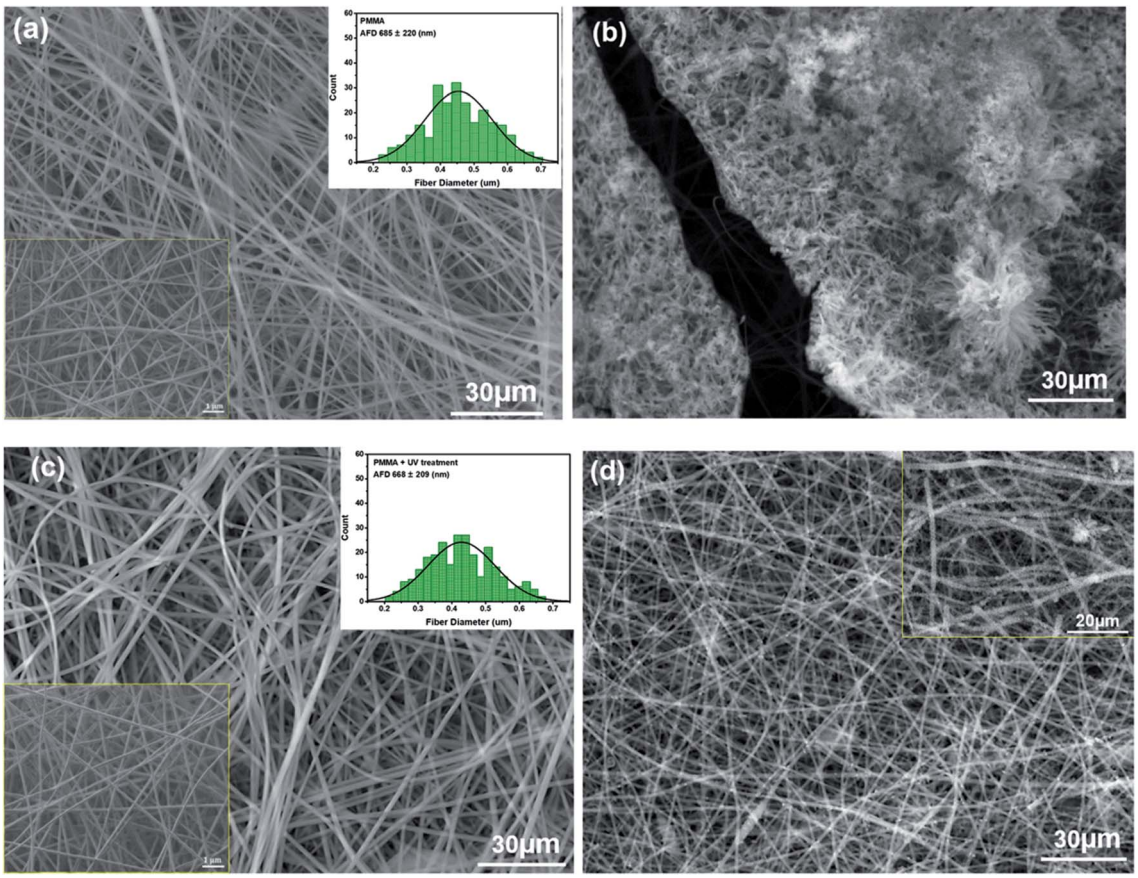

Fig. 1 (a) An SEM image of PMMA nanofibers and the distribution of their diameters (the inset shows an SEM image at higher magnification). (b) An SEM image of PMMA after the deposition of AmG/PANI. (c) An SEM image of PMMA after UV treatment and the distribution of PMMA fiber diameters (the inset shows an SEM image with higher magnification). (d) An SEM image of PMMA nanofibers after UV treatment and the deposition of AmG/PANI.

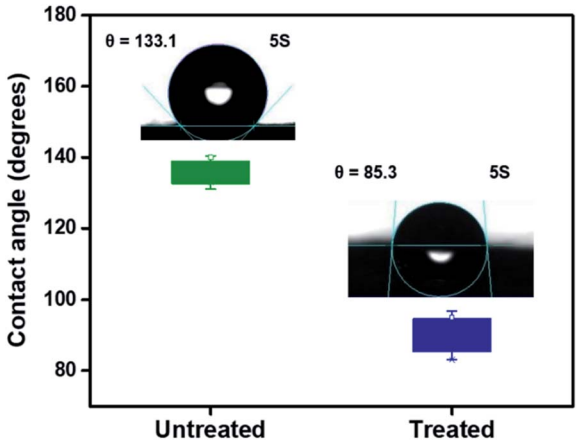

Fig. 2 Water contact angles of untreated and treated PMMA nanofiber surfaces.

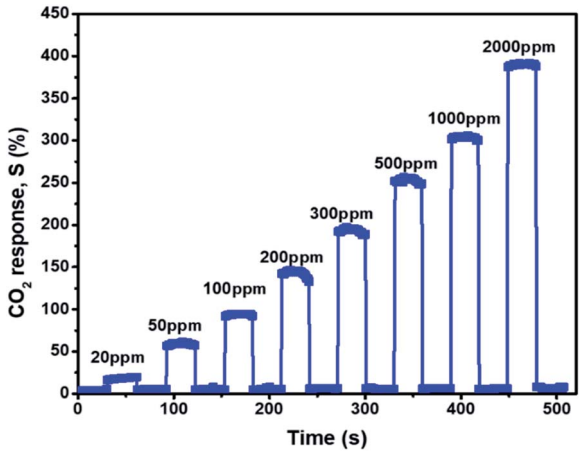

Fig. 3 The response of the AmG/PANI nanofiber gas sensor to different CO_2 concentrations.

surface by oxidizing it, resulting in carboxylic acid groups, and increased the radical oxygen content of the exposed surface, causing the nanofiber surface to become more hydrophilic.[30–32] While UV treatment modified the PMMA nanofiber surfaces, no remarkable changes in nanofiber morphology (668 ± 209 nm) were observed (Fig. 1c). As shown in Fig. 1d, AmG/PANI was uniformly dispersed in the PMMA nanofibers, indicating that UV treatment reduced the hydrophobicity of the PMMA surface by introducing oxidized groups onto the nanofiber surfaces. Similar results regarding the surface oxidation of PMMA have been previously reported.[33–35]

Contact angle measurements were performed on the PMMA nanofibers before and after UV treatment to study the surface wettability of the PMMA nanofibers. As shown in Fig. 2, the contact angle of PMMA nanofibers before UV irradiation was 133.1°. After UV treatment, the contact angle was significantly decreased to 85.3°, indicating better wettability. The results suggest that UV radiation enhanced the wettability of the PMMA nanofibers by introducing active sites onto the nanofiber surfaces.[29] These results agree with the SEM results discussed above.

Gas sensing properties of AmG/PANI nanofiber composites

A flexible nanofiber composite sensor was placed in the sensing chamber to observe its sensing behavior toward CO_2 gas at room temperature. Fig. 3 shows the response of the AmG/PANI nanofiber composite. The response increased dramatically when exposed to various concentrations of CO_2 ranging from 20 to 2000 ppm and recovered to the original value when the CO_2 was replaced by N_2.

The sensing results are similar to other results reported for CO_2 sensors based on π-conjugated amine (NBA) and zinc oxide (ZnO) nanohybrids,[25] polyethylenimine,[37] graphene (G) and aluminum oxide (Al_2O_3) quantum dot composites,[38] G/antimony oxide (Sb_2O_3) quantum dot composites,[39] and G/PANI/polystyrene (PS) nanocomposite films.[40] The high sensitivity of the AmG/PANI nanofiber composite for CO_2 is attributed to the formation of the carbamate moiety, which is the basis of the reversible CO_2 response that occurs more efficiently at lower temperatures.

The sensing properties of the AmG/PANI and PANI nanofiber composites for 20 ppm CO_2 gas were investigated. Fig. 4a shows the responses of the AmG/PANI and PANI nanofiber gas sensors

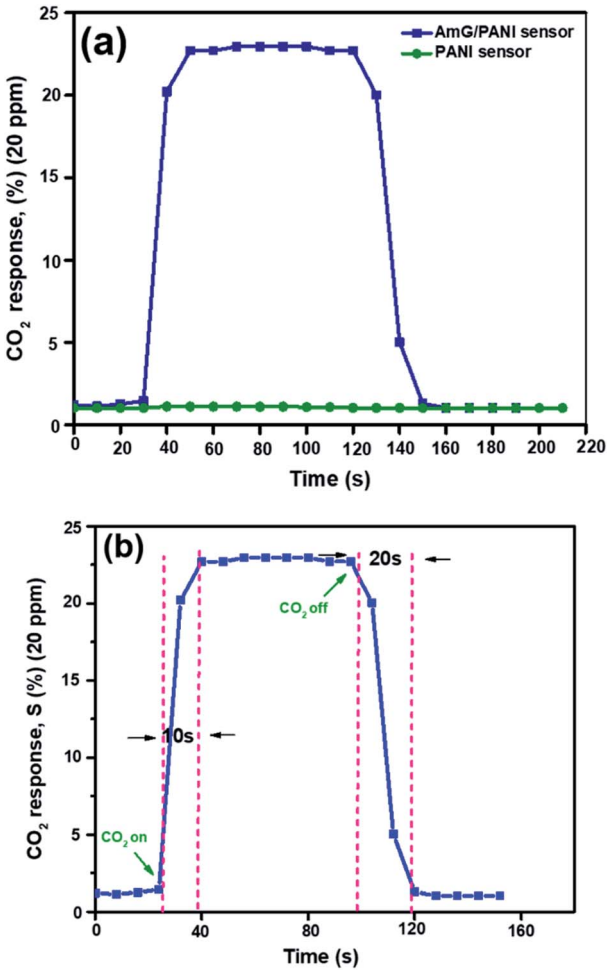

Fig. 4 (a) The dynamic responses of the two types of sensor to 20 ppm CO_2 gas. (b) The response and recovery characteristics of a single cycle for the AmG/PANI nanofiber gas sensor to 20 ppm CO_2 gas.

Table 1 Comparison of the performances of the AmG/PANI sensor with other sensors reported in the literature

Material	CO_2 concentration (ppm)	Response time (s)	Recovery time (s)	Temp. (°C)	Ref.
AmG/PANI nanofiber composite	20	10	20	RT	This work
NBA/ZnO nanohybrids	500	206	354	RT	25
G/Sb_2O_3 composite	50	16	22	RT	42
G/PANI/PS nanocomposite	20	65	65	RT	43
Carbon nanotube (CNT) thin film	800	>20	>75	RT	44

toward 20 ppm of CO_2 at room temperature. The PANI nanofiber-based sensor exhibited no sensitivity to CO_2 gas at 20 ppm, unlike the sensor based on AmG/PANI nanofibers. Fig. 4b shows the response and recovery characteristics of a single cycle for the AmG/PANI nanofiber gas sensor for 20 ppm of CO_2 gas. The time required for resistance to increase to 90% of the highest value is known as the response time of the gas sensor. The time required for the resistance to decrease from 90% of the highest value to the initial resistance value is known as the recovery time. The response and recovery times of the AmG/PANI nanofiber gas sensor were approximately 10 and 20 s, respectively, much better than those reported for other CO_2 sensors (Table 1).

Table 1 shows that our sensor showed a higher sensitivity toward CO_2 at room temperature compared to other reported CO_2 sensors, with the exception of G/PANI/PS nanocomposite sensors. However, our response and recovery times were much better, as mentioned above.

The bar plot in Fig. 5 illustrates the selectivity of the sensor for the detection of CO_2 over carbon monoxide (CO), ammonia (NH_3), and hydrogen (H_2) at concentrations of 100 ppm. The sensor showed extreme selectivity to CO_2 compared to the other gases at the same concentration. Mandal *et al.*[25] reported a high selectivity at 5000 ppm using NH_3, CO, and H_2S gases. A similar result was obtained in this study but at a considerably lower ppm.

The stability of the AmG/PANI nanofiber gas sensor was examined for 30 days. Good stability is essential for the use of the sensor in practical applications. Fig. 6 presents the stability of the AmG/PANI sensor exposed to 300 ppm of CO_2 for 30 days. The stability was evaluated each day for 10 days. After observing no change in sensitivity for 10 days, the stability was then tested every three days. The results clearly indicate that the sensor exhibited nearly constant sensing signals for one month.

The excellent sensing properties of the AmG/PANI nanofiber composite toward CO_2 gas can be attributed to the following two mechanisms. Usually, of the three classes of amine, primary amines react with CO_2 to produce carbamates. The reaction mechanism of CO_2 with primary amine to form carbamates is shown in eqn (1):

$$CO_2 + 2RNH_2 \leftrightarrow RNHCOO^- + RNH_3^+. \quad (1)$$

Theoretically, two primary amines are needed to trap CO_2.[24] First, a lone pair of amine electrons attaches to the carbon atom of CO_2 to form a zwitterion. Next, another free amine deprotonates the zwitterion to form the carbamate. Caplow *et al.*[36] were the first to describe the zwitterionic mechanism in the formation of carbamate from the interaction between the primary amine and CO_2. During this reaction, the number of free amines is reduced, and the proton mobility is subsequently reduced, which in turn increases the resistance.[37,38] In the second mechanism, the p-type PANI and n-type AmG in the AmG/PANI nanofiber composite form a p–n junction at the interface between them.[39,40] Consequently, a depletion layer is

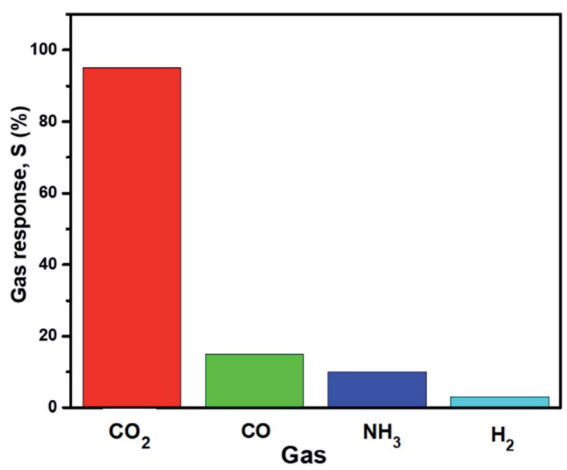

Fig. 5 The selectivity of the AmG/PANI nanofiber composite gas sensor to various gases at concentrations of 100 ppm.

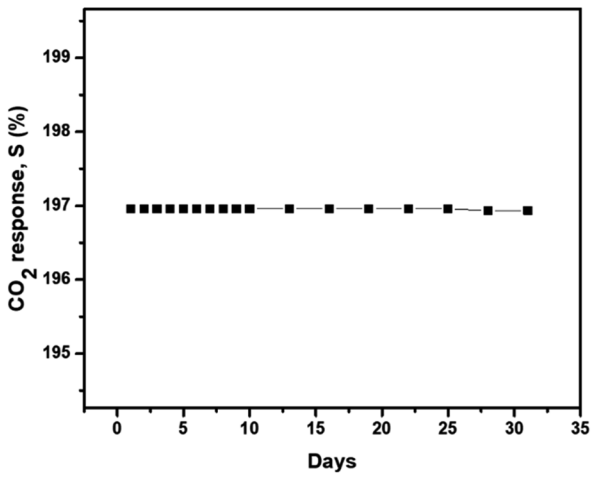

Fig. 6 The long-term stability of the AmG/PANI nanofiber composite gas sensor when exposed to 300 ppm CO_2.

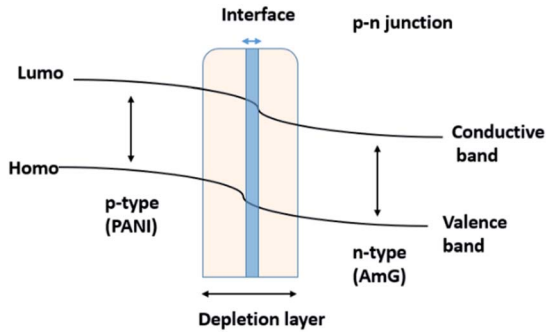

Fig. 7 A schematic illustration of the formation of the p–n junction between p-type PANI and n-type AmG.

formed at the interface.[40,41] Fig. 7 schematically shows the formation of the p–n junction between p-type PANI and n-type AmG. When CO_2 gas is injected into the chamber, the gas molecules are adsorbed by the surface of the AmG/PANI nanofiber composite. When the electrons are released at the junction into PANI, the majority carriers (holes) in PANI are compensated, which might increase the thickness of the depletion layer. This further increases the resistance of the AmG/PANI sensor in the presence of CO_2.[25,41] Thus, the enhanced CO_2 sensing properties of the AmG/PANI nanofiber sensor can be attributed to the presence of the primary amine functional group and the p–n junction between p-type PANI and n-type AmG.

Conclusions

In summary, we designed and synthesized a CO_2 gas sensor *via* chemical polymerization using PMMA nanofibers as a flexible substrate and AmG/PANI as an active material. The fabricated sensors exhibited good CO_2 sensing properties at room temperature, fast response and recovery times (10 and 20 s, respectively), and good stability. The easy preparation and excellent properties of AmG/PANI suggest the viability of electrospun nanofibers as gas sensing materials. The sensing mechanisms of the AmG/PANI nanofiber sensor toward CO_2 were discussed. The results demonstrate that AmG/PANI/PMMA nanofiber composites are promising candidates for practical CO_2 sensors.

Experimental section

Materials

AmG was synthesized in our lab. GO, aniline (ACS reagent, ≥99.5%), *N*,*N*-dimethylformamide (DMF, 99.8%), PMMA (M_w = 996 000 g mol^{-1}), ethylenediamine (EDA, ≥99%), ammonium persulfate (APS, ≥98.0%), and 5-sulfosalicylic acid dihydrate (SSA, ≥99%) were obtained from Sigma-Aldrich (Oakville, ON, Canada). Deionized (DI) water was used in all experiments.

Synthesis of amino-functionalized graphene

GO was reduced by thermal annealing, as reported previously.[27] Briefly, reduced GO (200 mg) was dispersed in 15 mL of EDA in a vessel under vigorous stirring for 24 h under reflux at 80 °C. The AmG was then isolated by centrifugation and washed thoroughly with DI water, filtered, and dried in a vacuum oven at 80 °C for 24 h.

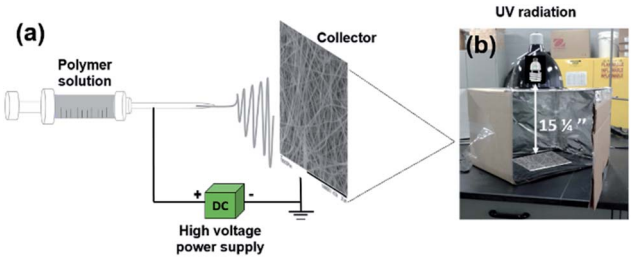

Fig. 8 (a) A schematic illustration of the electrospinning setup consisting of a power supply, syringe, and conducting collector. (b) Homemade setup for UV irradiation.

Preparation of PMMA nanofibers by electrospinning

A homogeneous dispersion of 1.06 g PMMA in 20 g DMF was electrospun using a homemade horizontal setup (see Fig. 8a). The setup consisted of a 5 mL glass syringe, a metallic needle (inner diameter = 0.84 mm; Cadence Science, Cranston, RI, USA), a syringe pump (PHD 2000; Harvard Apparatus, Holliston, MA, USA), and a high-voltage power supply (ES60P-5W; Gamma High Voltage Research Inc, Omaha Beach, FL, USA). The PMMA solutions were electrospun at room temperature for 24 h using a positive voltage of 27 kV, a working distance of 20 cm (distance between the needle tip and the collecting plate), and a solution feed rate of 0.6 mL h^{-1}. The nanofibers were collected continuously until mats of nanofibers with a thicknesses of approximately 0.75 mm were formed.

UV radiation treatment. The PMMA nanofiber mats were cut into square pieces (40 × 40 mm) and exposed to UV radiation in a homemade setup. The distance between the UV radiation source and the mat was 15.25 inches, as shown in Fig. 8b. The PMMA electrospun nanofibers were subjected to UV radiation at a wavelength of 365 nm for different exposure times (10 and 20 min). The radiation time of 10 min was chosen for subsequent experiments.

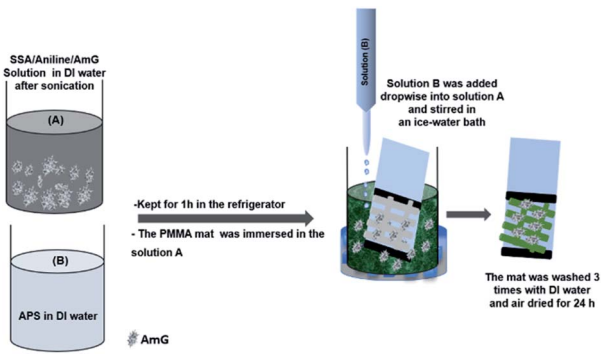

Fig. 9 A schematic illustration of the fabrication process of the AmG/PANI/PMMA nanofiber sensor.

Sensor fabrication of sensors

Treated and untreated PMMA nanofiber mats were fixed to Teflon films (25 × 25 mm) using adhesive tape. AmG/PANI was then grown on the surface of electrospun PMMA nanofibers *via in situ* polymerization. Fig. 9 schematically illustrates the fabrication process of the AmG/PANI/PMMA nanofiber composite sensors. First, 10 mg AmG was dispersed in 50 mL DI water by sonication for 1 h. Next, 2.45 g SSA and 1.86 g aniline were dissolved and mechanically stirred for 30 min to form solution A, while 4.45 g APS was dissolved in 50 mL DI water and stirred constantly for 30 min to form solution B. Solutions A and B were kept for 1 h in the refrigerator at 5 °C. Subsequently, the PMMA nanofiber mats were immersed in solution A. Solution B was then added dropwise into solution A followed by stirring in an ice-water bath for different polymerization times (1, 2, and 4 h). The polymerization time of 1 h was chosen for further experiments. Subsequently, the nanofiber mats were removed from the solution, washed with a large amount of DI water, and washed several times with ethanol to remove the residual oxidant. Finally, all nanofiber composites were dried at room temperature. Solutions A and B solutions were similarly prepared without the addition of AmG for comparative analysis. Copper tape was used as an electrode on the two opposite ends of a Teflon film for electrical connection. The sensors were stored at room temperature under vacuum until their sensing properties were tested.

Measurements

To study the morphologies of the PMMA nanofibers before and after UV treatment, the PANI/PMMA and AmG/PANI/PMMA nanofiber composites were examined using a table-top scanning electron microscope (TM3030 plus, Toshiba, Rexdale, ON, Canada) without any metallic coating. The fiber diameters were determined using Image-Pro Plus® software. Approximately 900 nanofibers were randomly selected from three independent SEM images (300 from each specimen) and used for analysis. Contact angle measurements were carried out using the sessile drop method at room temperature under atmospheric conditions with n OCA contact angle system (DataPhysics Instruments GmbH, Filderstadt, Germany) in combination with SCA 20 software (Dataphysics Instruments) for image analysis and contact angle calculation. A small volume (2 μL) of water was pipetted onto the nanofiber surface. Images were automatically taken as function of time. The reported contact angles are the average of five measurements taken at different positions on each sample.

To characterize the performance of the fabricated AmG/PANI/PMMA nanofiber composites as a CO_2 sensor, the sensor resistance values were recorded using a PalmSens3 instrument (PalmSens EmStat+Potentiostat w/Bluetooth, Compact Electrochemical interfaces, BASi®, West Lafayette, IN, USA) upon exposure to CO_2 gas at different concentrations (see Fig. 10). The flow rates of CO_2 and nitrogen were controlled by mass flow controllers (MKS instruments Inc., 1179C mass-flow®, Kanata, ON, Canada). The concentration of CO_2 gas was varied from 20 to 2000 ppm by adjusting the flow rates of CO_2 and nitrogen. The sensitivity of the sensor was investigated in a square, sealed, glass test chamber with a gas inlet and gas outlet along with electrical connections. When the sensor resistance was stable, CO_2 gas was injected into the test chamber *via* a micro-injector through a rubber plug. After the resistance reached a new value, nitrogen gas was injected into the test chamber for gas sensor recovery. The sensitivity (response) of the sensor was defined as the ratio of the change in the resistance S:

$$S\,(\%) = (R_{\text{gas}} - R_{\text{N}_2 \text{ or air}})/R_{\text{N}_2 \text{ or air}} \times 100, \quad (2)$$

where $R_{\text{N}_2 \text{ or air}}$ is the initial resistance obtained using N_2 or air as the base gas, respectively, and R_{gas} is the resistance of the sensor in CO_2.

The response (recovery) time is the time taken for the sensor to achieve a minimum of 90% of the total resistance change in the case of adsorption (desorption). All experiments were conducted at room temperature, and the relative humidity within the chamber was the same as the ambient relative humidity, which was between 30% and 35% during measurement.

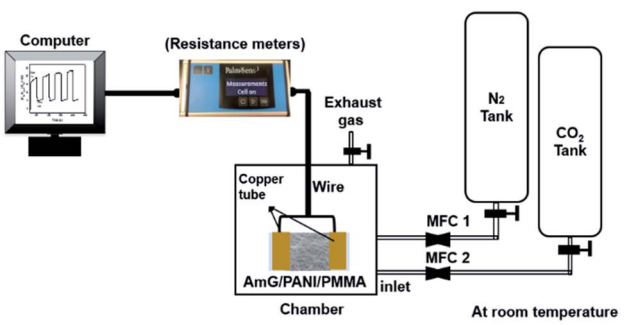

Fig. 10 A schematic diagram of the gas sensing measurements.

Author contributions

Hanan Abdali designed the study, performed the experiments, collected test data, interpreted results, and drafted the manuscript. Bentolhoda Heli helped perform the experiments and interpret the results. Abdellah Ajji designed the study, interpreted the results, and reviewed and edited the manuscript.

Conflicts of interest

There are no conflicts to declare.

Acknowledgements

This research was supported by the National Science and Engineering Research Council of Canada. The authors thank the Ministry of Education for their financial support of Hanan Abdali. The authors also thank Mr Sébastien Chenard for his invaluable help in constructing the gas detection setup. The authors are grateful to Mrs Claire Cerclé and Mr Matthieu Gauthier for their kind help during this study. Finally, the

authors acknowledge the reviewers of RSC Advances for their invaluable comments in improving this manuscript.

References

1 C. E. Booth, D. G. McDonald and P. J. Walsh, Acid-base balance in the sea mussel, Mytilus edulis. I. Effects of hypoxia and air-exposure on hemolymph acid-base status, *Mar. Biol. Lett.*, 1984, **5**, 347–358.

2 R. Desai, *et al.*, Indium sesquitelluride (In_2Te_3) thin film gas sensor for detection of carbon dioxide, *Sens. Actuators, B*, 2005, **107**(2), 523–527.

3 G. G. Mandayo, *et al.*, Performance of a CO_2 impedimetric sensor prototype for air quality monitoring, *Sensors*, 2011, **11**(5), 5047–5057.

4 J. Herrán, G. G. Mandayo and E. Castano, Solid state gas sensor for fast carbon dioxide detection, *Sens. Actuators, B*, 2008, **129**(2), 705–709.

5 C.-J. Chiang, *et al.*, *In situ* fabrication of conducting polymer composite film as a chemical resistive CO_2 gas sensor, *Microelectron. Eng.*, 2013, **111**, 409–415.

6 C. Wang, *et al.*, Metal oxide gas sensors: sensitivity and influencing factors, *Sensors*, 2010, **10**(3), 2088–2106.

7 S. Park, C. Park and H. Yoon, Chemo-electrical gas sensors based on conducting polymer hybrids, *Polymers*, 2017, **9**(5), 155.

8 E. Llobet, Gas sensors using carbon nanomaterials: a review, *Sens. Actuators, B*, 2013, **179**, 32–45.

9 T. T. Tung, *et al.*, Recent advances in sensing applications of graphene assemblies and their composites, *Adv. Funct. Mater.*, 2017, **27**(46), 1702891.

10 K. S. Novoselov, *et al.*, Two-dimensional gas of massless Dirac fermions in graphene, *Nature*, 2005, **438**(7065), 197.

11 K. S. Novoselov, *et al.*, Electric field effect in atomically thin carbon films, *Science*, 2004, **306**(5696), 666–669.

12 C. Lee, *et al.*, Measurement of the elastic properties and intrinsic strength of monolayer graphene, *science*, 2008, **321**(5887), 385–388.

13 A. A. Balandin, *et al.*, Superior thermal conductivity of single-layer graphene, *Nano Lett.*, 2008, **8**(3), 902–907.

14 J. Du and H. M. Cheng, The fabrication, properties, and uses of graphene/polymer composites, *Macromol. Chem. Phys.*, 2012, **213**(10–11), 1060–1077.

15 T. Kuila, *et al.*, Chemical functionalization of graphene and its applications, *Prog. Mater. Sci.*, 2012, **57**(7), 1061–1105.

16 D. Cai and M. Song, Recent advance in functionalized graphene/polymer nanocomposites, *J. Mater. Chem.*, 2010, **20**(37), 7906–7915.

17 C. Bao, *et al.*, *In situ* preparation of functionalized graphene oxide/epoxy nanocomposites with effective reinforcements, *J. Mater. Chem.*, 2011, **21**(35), 13290–13298.

18 M. Ioniță, *et al.*, Graphene and functionalized graphene: extraordinary prospects for nanobiocomposite materials, *Composites, Part B*, 2017, **121**, 34–57.

19 J. Xu, Y. Wang and S. Hu, Nanocomposites of graphene and graphene oxides: synthesis, molecular functionalization and application in electrochemical sensors and biosensors. A review, *Microchim. Acta*, 2017, **184**(1), 1–44.

20 K. Hu, *et al.*, Graphene-polymer nanocomposites for structural and functional applications, *Prog. Polym. Sci.*, 2014, **39**(11), 1934–1972.

21 H. J. Salavagione, Promising alternative routes for graphene production and functionalization, *J. Mater. Chem. A*, 2014, **2**(20), 7138–7146.

22 V. Georgakilas, *et al.*, Functionalization of graphene: covalent and non-covalent approaches, derivatives and applications, *Chem. Rev.*, 2012, **112**(11), 6156–6214.

23 Y. G. Ko, S. S. Shin and U. S. Choi, Primary, secondary, and tertiary amines for CO_2 capture: designing for mesoporous CO_2 adsorbents, *J. Colloid Interface Sci.*, 2011, **361**(2), 594–602.

24 S. Stegmeier, *et al.*, Mechanism of the interaction of CO_2 and humidity with primary amino group systems for room temperature CO_2 sensors, *Procedia Chem.*, 2009, **1**(1), 236–239.

25 B. Mandal, *et al.*, π-Conjugated Amine–ZnO Nanohybrids for the Selective Detection of CO_2 Gas at Room Temperature, *ACS Appl. Nano Mater.*, 2018, **1**(12), 6912–6921.

26 S.-A. Chen and G.-W. Hwang, Structures and properties of the water-soluble self-acid-doped conducting polymer blends: sulfonic acid ring-substituted polyaniline/poly(vinyl alcohol) and poly (aniline-co-*N*-propanesulfonic acid aniline)/poly(vinyl alcohol), *Polymer*, 1997, **38**(13), 3333–3346.

27 H. Abdali and A. Ajji, Preparation of Electrospun Nanocomposite Nanofibers of Polyaniline/Poly(methyl methacrylate) with Amino-Functionalized Graphene, *Polymers*, 2017, **9**(9), 453.

28 A. Polini, *et al.*, Collagen-functionalised electrospun polymer fibers for bioengineering applications, *Soft Matter*, 2010, **6**(8), 1668–1674.

29 A. Rabiatul, *et al.*, Surface modification of electrospun poly(methyl methacrylate) (PMMA) nanofibers for the development of *in vitro* respiratory epithelium model, *J. Biomater. Sci., Polym. Ed.*, 2015, **26**(17), 1297–1311.

30 I. Pashkuleva, *et al.*, Surface modification of starch based biomaterials by oxygen plasma or UV-irradiation, *J. Mater. Sci.: Mater. Med.*, 2010, **21**(1), 21–32.

31 A. Yusilawati, *et al.*, Surface modification of polystyrene beads by ultraviolet/ozone treatment and its effect on gelatin coating, *Am. J. Appl. Sci.*, 2010, **7**(6), 724.

32 J. M. Goddard and J. Hotchkiss, Polymer surface modification for the attachment of bioactive compounds, *Prog. Polym. Sci.*, 2007, **32**(7), 698–725.

33 Y. Dekhtyar, *et al.*, Surface properties of ocular prostheses material change under UV influence, in *5th European Conference of the International Federation for Medical and Biological Engineering*, Springer, 2011.

34 A. Nematollahzadeh, *et al.*, Increasing the interfacial adhesion in poly(methyl methacrylate)/carbon fibre composites by laser surface treatment, *Polym. Polym. Compos.*, 2006, **14**(6), 585–589.

35 D. Rymuszka, *et al.*, Changes in surface properties of polymethylmethacrylate (PMMA) treated with air plasma, *Ann. UMCS, Chem.*, 2015, **70**(1), 65–78.
36 M. Caplow, Kinetics of carbamate formation and breakdown, *J. Am. Chem. Soc.*, 1968, **90**(24), 6795–6803.
37 S. Choi, J. H. Drese and C. W. Jones, Adsorbent materials for carbon dioxide capture from large anthropogenic point sources, *ChemSusChem*, 2009, **2**(9), 796–854.
38 T. C. Doan, *et al.*, Carbon dioxide detection with polyethylenimine blended with polyelectrolytes, *Sens. Actuators, B*, 2014, **201**, 452–459.
39 D. Majumdar, Functionalized-Graphene/Polyaniline Nanocomposites as Proficient Energy Storage Material: An Overview, *Innov. Energy Res.*, 2016, **5**(145), DOI: 10.4172/2576-1463.1000145.
40 H. Tai, *et al.*, Fabrication and gas sensitivity of polyaniline–titanium dioxide nanocomposite thin film, *Sens. Actuators, B*, 2007, **125**(2), 644–650.
41 J. Sun, *et al.*, Preparation of polypyrrole@WO_3 hybrids with pn heterojunction and sensing performance to triethylamine at room temperature, *Sens. Actuators, B*, 2017, **238**, 510–517.
42 K. Nemade and S. Waghuley, Role of defects concentration on optical and carbon dioxide gas sensing properties of Sb_2O_3/graphene composites, *Opt. Mater.*, 2014, **36**(3), 712–716.
43 J. Bhadra, *et al.*, Fabrication of polyaniline–graphene/polystyrene nanocomposites for flexible gas sensors, *RSC Adv.*, 2019, **9**(22), 12496–12506.
44 Z.-D. Lin, S.-J. Young and S.-J. Chang, CO_2 gas sensors based on carbon nanotube thin films using a simple transfer method on flexible substrate, *IEEE Sens. J.*, 2015, **15**(12), 7017–7020.